The critical bubble diameter of the lift force in technical and environmental, buoyancy-driven bubbly flows

Ziegenhein, T.; Lucas, D.;

Originally published:

April 2019

International Journal of Multiphase Flow 116(2019), 26-38

DOI: https://doi.org/10.1016/j.ijmultiphaseflow.2019.03.007

Perma-Link to Publication Repository of HZDR:

https://www.hzdr.de/publications/Publ-26509

The critical bubble diameter of the lift force in bubble columns

T. Ziegenhein*, D. Lucas

Helmholtz-Zentrum Dresden-Rossendorf e.V., 01314 Dresden, Germany

* Corresponding author. Tel.: +49 3512602503; fax: +49 3512603440.
E-mail address: t.ziegenhein@hzdr.de (Thomas Ziegenhein).

Abstract

The lift force as part of the so-called non-drag forces influences distinctly the span-wise gas void fraction in bubbly flows. Towards larger bubble sizes, experiments at single bubbles show that the lift force changes its sign at a critical diameter. This effect would cause a separation of small and large bubbles in bubbly flows when a liquid velocity profile with gradients is present. In the present work, this separation is studied for different bubble columns setups in order to identify such a critical diameter. For all setups, almost the same critical diameter is found. Since the lift force is the only known force that could cause a separation of different bubble sizes, it can be concluded that the found critical diameter is indeed the diameter at which the lift force changes its sign. Therefore, a simple method is obtained with which the sign change of the lift force can be determined under realistic flow conditions.

Keywords: Lift force, bubbly flows, critical diameter, bubble column

1 Introduction

In almost all applications that deal with bubbly flows, a polydispersed size distribution can be found. Since the forces acting on bubbles are changing with the bubble size, very complex phenomena can be observed in such flows. In this context, the lateral bubble forces are very important since they determine the local bubble size distribution. In particular the lift force seems to play a major role because a sign change occurs which would separate small and big bubbles. This separation is vital to understand complex effects; for example, it might cause the regime transition in bubble columns (Lucas et al. 2005) for which up to now only empirical correlations exists.

Despite its importance, the lift force is not yet well understood; measurements are very rare due complex effects. Nevertheless, measurements in high viscous systems are possible due to the rotating belt experiment of Kariyasaki (1987), which was used by Tomiyama et al. (2002) to formulate the well-known empirical Tomiyama correlation. These measurements were recently extended by Aoyama (2017) who revealed a more complex behavior of the lift coefficient than expected. Under industrial relevant conditions that usually use medium to low viscous systems, however, the rotating belt cannot be used. This gap was recently closed by Ziegenhein et al. (2017) with an averaging procedure and a new experimental method.

All experiments revealed a sign change of the lift coefficient towards larger bubbles. This behavior was also confirmed with Direct Numerical Simulations (DNS) by, for example, Ervin & Tryggvason (1997), Bothe et al. (2006), or Dijkhuizen et al. (2010). However, determining the critical diameter is costly with the existing experiments as well as DNS since it has to be determined iteratively. This becomes in particular crucial for wobbling bubbles since a long measuring/simulation time is needed. Besides the practical problem of generating a constant bubble size under turbulent conditions over a long time, all documented experimental and simulation results scatter more or less. Therefore, an exact measurement of the critical diameter is often connected to many experiments and/or a fit through available measuring points.

The present work aims to provide a simple method to determine the critical diameter at which the lift force is changing. The principle idea is based on the work of Lucas and Tomiyama (2011) who used the separation of different sized bubbles over the height in vertical pipe-flows to prove the existence of the lift force under turbulent conditions. We will use a bubble column in which the bubbles separate depending on their size. Identifying a homogenous distribution of bubbles of a certain size over the cross section will allow us to identify the critical diameter. This method is discussed in detail and results are shown for six different experimental conditions. With the help of the following set of dimensionless numbers

$$Eo = \frac{\Delta\rho g d_B^2}{\sigma}, Eo_\perp = \frac{\Delta\rho g d_\perp^2}{\sigma}, Re_B = \frac{\rho v_{rel} d_B}{\mu}, Re_\perp = \frac{\rho v_{rel} d_\perp}{\mu}, Mo = \frac{g\mu^4\Delta\rho}{\rho^2\sigma^3}, \qquad (1)$$

the results are compared to the literature.

2 Experimental Setup

The experimental setup consists of a tall bubble column with six holes for spargers, which are grouped to Group 1 (G1) and Group 2 (G2). Two sparger setups are used in the present study, the Small (S) setup consists of 0.12 mm inner-diameter needles in G1 and 0.6 mm in G2. In the Normal (N) setup, the 0.12 mm needles are replaced with 0.3 mm in G1. The total gas volume flow is 1 l/min at standard conditions for all setups. The gas volume flow is distributed differently over G1 and G2 by using two mass flow controllers. In the following, the operation points will be named with the sparger setup followed by the percentage of the gas volume flow through G1, e.g. N70 for the 0.3mm/0.6mm needle setup and 70% gas volume flow through G1. The fill height of the column was with 1.8 m constant for all operation points.

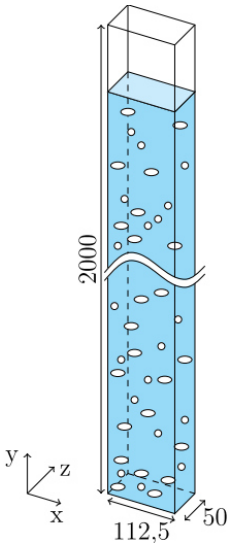

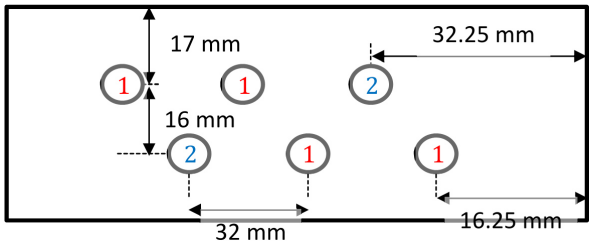

→Flow l/min Needle size ↓	G1:0.7 G2:0.3	G1:0.6 G2:0.4	G1:0.55 G2:0.45	G1:0.4 G2:0.6	G1:0.25 G2:0.75	G1:0.1 G2:0.9
G1: 0.12 mm G2: 0.6 mm		S60				
G1: 0.3 mm G2: 0.6 mm	N70		N55	N40	N25	N10

Figure 1 Experimental setup (left), sparger setup with sparger Group (G) enumeration (right top) and the operation points regarding different gas volume flows for the Small (S) needle setup and Normal (N) needle setup.

Bubbles are picked by hand from photographs, which had a resolution of 60 µm per pixel, with support of edge detecting algorithms. A set of ten photos was recorded every second with 250 frames per second. The evolution of bubble clusters over time is used to identify overlaid bubbles in such clusters. With this procedure, the bubble sizes were determined at four heights: 50 mm, 600 mm, 1200 mm and 1600 mm above the sparger. Per measuring height, 4000 bubbles were picked. The complete column was in the Depth of Field (DoF) of the camera setup so that all bubbles in depth direction are considered in the present work. A detailed description of the bubble picking method can be found in (Ziegenhein et al. 2016). The bubble size is defined in the present work as the spherical equivalent diameter of the volume equal to the solid of revolution of the projected bubble. Compared to the method of calculating the volume from the major and minor axis of the projected bubble, almost the same bubble size was obtained. In this context, the major axis is defined as the longest

possible chord of the projected bubble and the minor axis the longest chord perpendicular to the major axis. The definition of the major axis is also used to calculate the modified Eötvös and Reynolds number.

The liquid velocity was measured with Particle Tracking Velocimetry methods. The particles were identified with a Hough-like transformation. The tracking was realized with a brute-force method including a correction step. The flow was seeded with 50 µm Polyamide particles from DANTEC DYNAMICS A/S. Every second a set of four photos with 2500 frames per second was recorded. The resolution of the pictures taken was 10 µm/pixel; the total measuring time was 10 000 seconds at each measuring height. A detailed description of the particle identification and particle tracking can be found in (Hessenkemper & Ziegenhein 2017).

3 Method

The lift force depends on the gradient of the liquid velocity profile

$$F_{Lift} = -C_L \rho_L (\vec{u}_G - \vec{u}_L) \times rot(\vec{u}_L) \ . \quad (2)$$

Considering the lift force on a horizontal line in the center of the column and neglect the stream wise gradients, the time-averaged lateral velocities and the gradients in depth direction, only the sideward component of the lift force remains

$$F_{Lift,x} = -\rho_l C_L \left(u_{G,y} - u_{L,y}\right) \cdot \frac{du_{L,y}}{dx} \ . \quad (3)$$

The lift coefficient C_l has a critical diameter at which the sign is changed from positive, for small bubbles, to negative, for larger bubbles. For systems with a high Morton number, this sign change was proven by the experiments of Tomiyama et al. (Tomiyama et al. 2002), for moderate Morton numbers by the experiments of Aoyama et al. (2017), and for low Morton number systems by our own experiments (Ziegenhein et al. 2017). Therefore, in the present bubble column a separation of the small bubbles should occur when a velocity profile with significant gradients is present. At the different operation points, the velocity profiles are predominantly center-peaked (Figure 2 left); however, at operation point N55 we observed a double peaked velocity profile (Figure 2 right). Regardless of the shape of the velocity profile, due to the sign change of the lift force the smaller bubbles tend away from the velocity peak whereas the larger bubbles will accumulate at the peak.

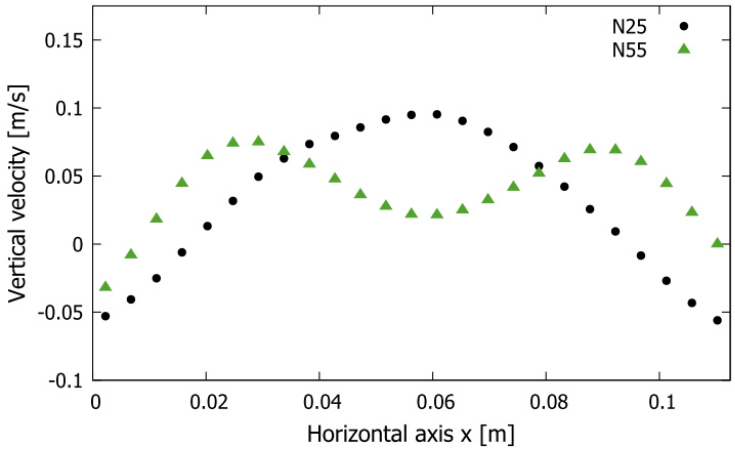

Figure 2 Velocity profile in the center of the bubble column 1600 mm above the sparger for operation point N25 and N55.

When a tall bubble column with a stable velocity profile is used, the bubbles have enough time to separate whereas the bubbles with a lift coefficient close to zero should be more or less distributed equally over the column cross section. The purpose is therefore to find these equally distributed bubbles. If these bubbles have all the same size, it can be concluded that this bubble size is the critical diameter at which the lift coefficient is changing its sign.

Since only a limited number of bubbles are available, we might not identify a specific size but a specific size range that contains the critical bubble diameter. Therefore, the bubble size distribution is separate in overlapping intervals of 0.5 mm size with an overlap of 0.49 mm. If the bubbles in an interval would be equally distributed, a flat void fraction would occur. The void fraction profile is simply calculated by dividing the width of the column in 10 cells, if a bubble of the present interval is inside the cell, the intersecting volume of the bubble and the cell will be added to a cell counter. Afterwards, the summed-up volume is divided by the cell volume and the number of pictures evaluated. With this method, a void fraction profile can be described for each interval. Whether a profile is flat is decided by the normalized standard deviation of the void fraction over the width; a flat profile would have a standard deviation of zero. For each interval a Sauter diameter can be calculated, to which is referred in the following.

This procedure is exemplary shown for operation point N25 in Figure 3. On the left side, the normalized standard deviation is shown with respect to the Sauter diameter of the bubbles inside the 0.5 mm large intervals. A clear minimum between 5.05 and 5.15 mm is observed. Looking at the gas void fraction profiles, which are normalized with their averaged value, the typical behavior of a center minimum and a wall peak for bubbles between 4.25 and 4.75 mm is seen. Bubbles in the range of 4.85 and 5.35 mm with a Sauter diameter of 5.05 mm show another behavior; still a center minimum is present but a wall peak is missing. Instead, the profiles show a slight peak near the maximum shear rate of the liquid velocity (Figure 2) at each side. These double peaks might be caused by bubbles with a small lift coefficient that are still traveling towards the center; due to the decreasing shear rate towards the center, they accumulate at points of lower shear rate. The center minimum vanishes further for bubbles in the interval between 4.93 and 5.43 mm. Bubbles between 5.23 and 5.73 mm already show the typical center-peaked profile, which is obvious for bubbles between 5.94 and 6.44 mm.

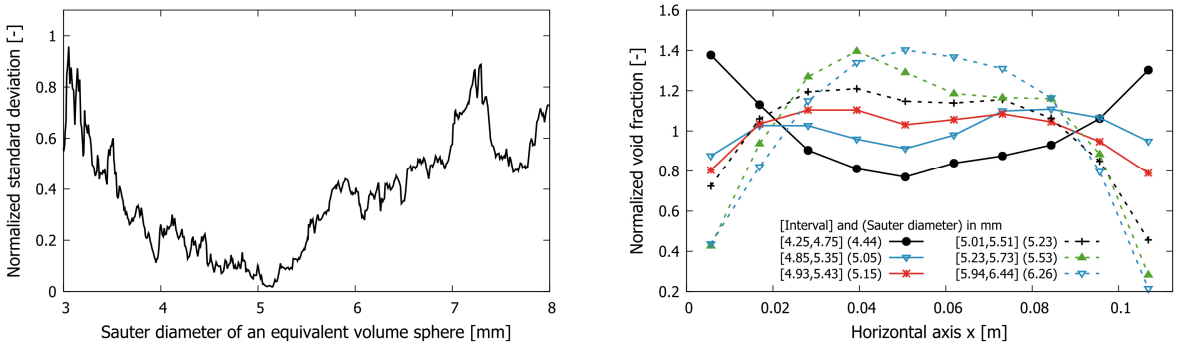

Figure 3 identifying the critical Sauter diameter for operation point N25. Left, the normalized standard deviation of the void fraction profiles; right, normalized void fraction profiles of different bubble sizes.

From the standard deviation and the void fraction profiles, the critical diameter of the lift force is between a Sauter diameter of 5.05 and 5.15 mm for the operation point N25. The size of this range might be determined by the available time the bubbles have to separate so that taller columns might have a better separation performance. For the other operation points, the critical diameter is likewise determined.

Noticeable is the operation point N55 with the stable velocity double peak (Figure 2). For this case, the large bubbles form a similar double peaked void fraction profile (Figure 4), as expected. The small bubbles form a complex void fraction profile with a center peak, a minimum at each velocity peaks, and an upward trend towards the wall. This behavior can be explained with the lift force model since the small bubbles with a positive lift coefficient migrate away from the two velocity maximums towards the center and the column walls.

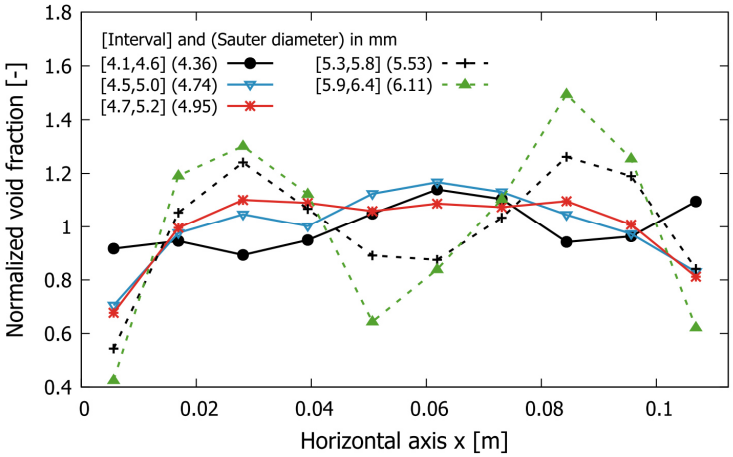

Figure 4 Normalized void fraction profiles for operation point N55.

To show that the spatial void distributions are not determined by the initial distribution at the sparger, the evolution along the column is studied (Figure 5). At the sparger (50 mm height) all profiles have a two-peaked void fraction profile, which is caused by the sparger setup. The asymmetric behavior, in particular for the small bubbles, might be due to a slightly different gassing of the needles, which might be explained by small manufacturing differences of the needles or an inhomogeneous gas distribution in the sparger system. More interesting is the fact that despite this more or less random gas distribution, the bubbles are sorting along the height. In particular, the interval from 4.25 mm to 4.75 mm, which is containing the bubbles with a probable positive lift coefficient, is developing over height from a more or less center-peaked profile to a profile with wall peaks. The bubbles in the interval from 4.93 to 5.43 mm, which is containing bubbles with a probable lift coefficient around zero, seem just to disperse over height. Finally, the large bubbles with a probable negative lift coefficient are migrating towards the center.

Statements on migrating bubbles are only meaningful if the bubble size distribution is not changing. One could imagine that the wall peaks of the interval containing the small bubbles emerge because the bubbles in the center coalesce to larger bubbles, which form a center peak thereby. An argument against this process is that the bubble size distribution (Figure 5) is relatively constant over height. In addition, from visual observations we could not see a significant break-up and/or coalescence behavior for the operation points around 1% gas hold up discussed here.

Summarizing, the following arguments support that we are able to determine the critical diameter of the lift force with the discussed method. First, a clear separation of the small and

big bubbles can be observed. Second, the lateral distribution over height is changing. Finally, the bubble size distribution is not distinctly changing. From these points, we can assume that the lift force separates the bubbles, depending on their lift coefficient. That the critical diameter we obtain with the described method is almost equal for the different operation points, as discussed in the next section, supports this assumption additionally.

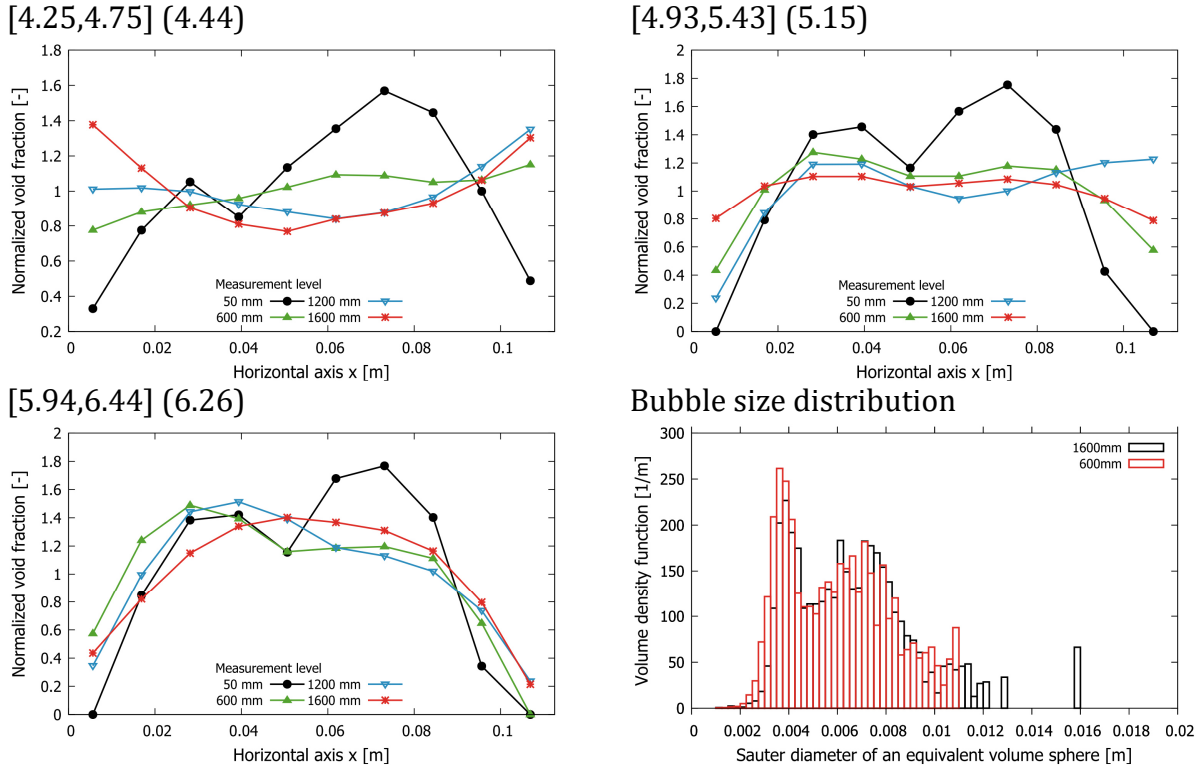

Figure 5 Evolution of the void fraction profiles over height for different diameters and the bubble size distribution at two different heights.

4 Results

The critical diameters obtained for the different operation points are around 5.14 mm (Figure 6). The separation performance, which is illustrated as error bar in Figure 6, is different for the different points, which might be due to different inlet conditions and therefore different flow situations. Overall, very similar results are obtained for different the operation points.

The characteristic length to describe the lift force, however, might not be the diameter of an equivalent sphere but the major axis of the bubble (Tomiyama et al. 2002) (Ziegenhein et al. 2017). A reasonable definition of the major axis might be the maximal chord of the projected bubbles. This length is for wobbling bubbles substantial larger than the horizontal axis due to deformation and rotation of the bubbles but equal for bubbles in high viscose/high Morton number systems. Our previous empirical correlation on bubble shapes obtained from several bubble column experiments (Ziegenhein & Lucas 2017) is well applicable for the present case (Figure 6). The average critical major axis is 6.3 mm for the average critical bubble diameter of 5.14 mm. If for every operation point the major axis is determined and afterwards averaged, the same result is obtained with a range of 6.2 to 6.35 mm.

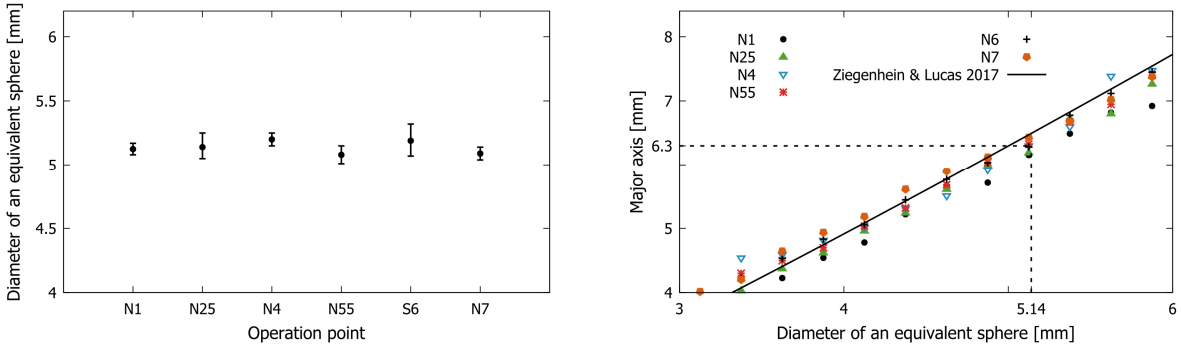

Figure 6 Results for all operations points (left). Determining the major axis of the average critical diameter (right).

Using the modified Eötvös number, which is calculated with major axis as length scale, the averaged critical Eötvös number of 5.4 fits very well to our previous lift force measurement (Ziegenhein et al. 2017) in the same air/water system Figure 7. In this work, we were able to quantify the lift force for different bubble sizes in very low Morton number systems with a new measuring method. Determining the exact critical Eötvös number at which the lift coefficient changes its sign with this method, however, is difficult. In addition, the result is close to the DNS of Dijkhuizen et al. (Dijkhuizen et al. 2010). Since Dijkhuizen et al. used the horizontal axis and not the major axis the DNS results might be in general under-predicted, which might explain the deviations. Surprisingly, also the empirical correlation of Tomiyama et al. (2002) is close to the present result despite their experiments were conducted in a very different bubble regime with high Morton numbers and very low Reynolds numbers from 1 – 10 compared to around 1000 in the present setup.

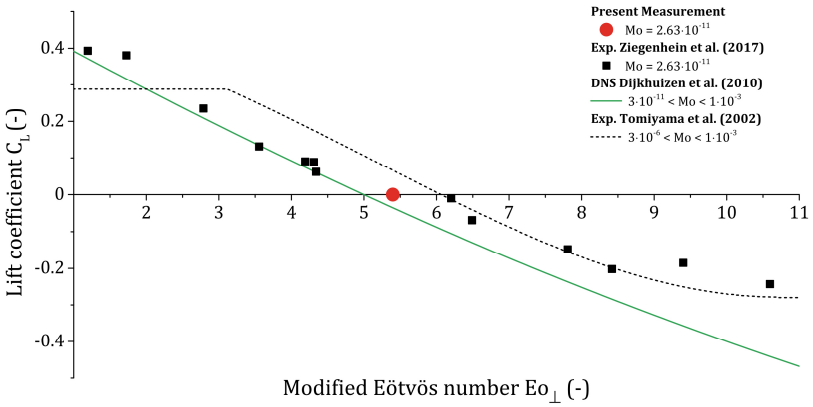

Figure 7 Present results compared to literature with respect to the modified Eötvös number.

That the critical modified Eötvös number obtained by Tomiyama et al. is close to the present results might be a happenstance as discussed by Aoyama et al. (2017) (Figure 8). They extended the experiments of Tomiyama et al. and found that the critical diameter is substantially changing when the Morton number is changing. The downward trend they described seems to reverse between a Morton number of 10^{-7} and 10^{-11}. Lucas and Tomiyama (2011) determined the critical diameter for steam/water systems and found an decreasing trend with lower Morton number. Nevertheless, their findings for a slightly smaller Morton number are close to our results.

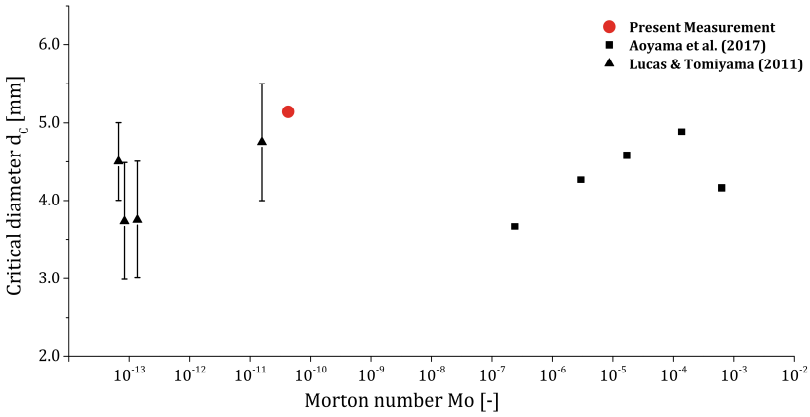

Figure 8 Present critical diameter compared to results from literature with respect to the Morton number.

5 Discussion

By investigating the separation of bubbles of different size along the height of a bubble column under different experimental conditions, we were able to determine a critical separation diameter. Smaller bubbles than this diameter tend to migrate away from peaks in the upward velocity profile, larger bubbles towards them. Considering the model of a shear induced lift force, this critical diameter is therefore the point where the lift coefficient has a sign change from positive to negative values. The determined critical diameter of 5.14 mm fit well to previous measurements in which the lift force was quantified. Therefore, it might be concluded that the findings from lift force measurements with single bubbles rising in an artificial shear field are applicable to bubbly flows in bubble columns at low void fractions.

Moreover, the importance of the lift force in bubble columns is underlined by the present study. Even with relatively small gradients in the liquid velocity profile, the separation of small and large bubbles is distinct. For modelling bubble columns, such a separation might be essential. In particular, the present findings might be important to understand regime transitions. With respect of simulating bubble columns with the two-fluid model, it must be carefully checked if the assumption of a mono-dispersed bubbly flow is valid. To describe the hydrodynamics correctly, several momentum equations for the gas phase should be considered.

6 References

Aoyama, S. et al., 2017. Lift force acting on single bubbles in linear shear flows. *International Journal of Multiphase Flow,* Volume 96, pp. 113-122.

Bothe, D., Schmidtke, M. & Warnecke, H.-J., 2006. VOF-Simulation of the Lift Force for Single Bubbles in a Simple Shear Flow. Chemical Engineering & Technology, Volume 29, p. 1048.

Dijkhuizen, W., van Sint Annaland, M. & Kuipers, J. A., 2010. Numerical and experimental investigation of the lift force on single bubbles. *Chemical Engineering Science,* Volume 65, pp. 1274–1287.

Ervin, E. A. & Tryggvason, G., 1997. The Rise of Bubbles in a Vertical Shear Flow. *Journal of Fluids Engineering,* Volume 119, p. 443.

Hessenkemper, H. & Ziegenhein, T., 2017. Shadowgraphy in bubbly flows. *International Journal of Multiphase Flow,* submitted.

Kariyasaki, A., 1987. *Behavior of a single gas bubble in a liquid flow with a linear velocity profile.* , Proceedings of the 1987 ASME/JSME Thermal Engineering Conference. No. 384.

Lucas, D., Prasser, H.-M. & Manera, A., 2005. Influence of the lift force on the stability of a bubble column. *Chemical Engineering Science,* Volume 60, pp. 3609 – 3619.

Lucas, D. & Tomiyama, A., 2011. On the role of the lateral lift force in poly-dispersed bubbly flows. *International Journal of Multiphase Flow,* Volume 37, p. 1178.

Tomiyama, A., Tamai, H., Zun, I. & Hosokawa, S., 2002. Transverse migration of single bubbles in simple shear flows. *Chemical Engineering Science ,* 57(11), pp. 1849-1858.

Ziegenhein, T. & Lucas, D., 2017. Observations on bubble shapes in bubble columns under different flow conditions. *Experimental Thermal and Fluid Science,* Volume 85, pp. 248-256.

Ziegenhein, T., Tomiyama, A. & Lucas, D., 2017. A new measuring concept to determine the lift force for distorted. *International Journal of Multiphase Flow,* submitted.

Ziegenhein, T., Zalucky, J., Rzehak, R. & Lucas, D., 2016. On the hydrodynamics of airlift reactors, Part I: Experiments. *Chemical Engineering Science,* Volume 150, pp. 54-65.